The Report Committee for Lee Michael Waters
Certifies that this is the approved version of the following report:

Annular Flow Regimes in a Novel Down-Hole Gas-Liquid Separator and Pump Connector

APPROVED BY
SUPERVISING COMMITTEE:

Supervisor:

Kamy Sepehrnoori

Co-Supervisor:

Paul M. Bommer

Annular Flow Regimes in a Novel Down-Hole Gas-Liquid Separator and Pump Connector

by

Lee Michael Waters

Report

Presented to the Faculty of the Graduate School of

The University of Texas at Austin

in Partial Fulfillment

of the Requirements

for the Degree of

Master of Science in Engineering

The University of Texas at Austin

December 2017

Acknowledgements

First and foremost, I would like to thank Dr. Bommer for providing me with the opportunity to conduct this research. During my time at The University of Texas at Austin, I was privileged to work with him in a variety of capacities: as a student; a teaching assistant; and a collaborator on this research. I cannot speak highly enough of Dr. Bommer and his quality as an educator. He made me feel welcome and made my time as a graduate student that much better. Thank you, Paul.

Additional thanks go to my colleague, Adi Suresh, Dr. Sepehrnoori for serving as a second reader, Daryl Nygaard for building the prototypes and troubleshooting most issues, Jessica Yeager for assistance in the reading room and Amy Stewart for academic advising. Finally, my deepest gratitude to Kelsey Hoffman for her unwavering support.

Abstract

Annular Flow Regimes in a Novel Down-Hole Gas-Liquid Separator and Pump Connector

Lee Michael Waters, M.S.E

The University of Texas at Austin, 2017

Supervisor: Kamy Sepehrnoori

Co-Supervisor: Paul M. Bommer

Flow patterns were investigated in a novel dual-use pump connector and down-hole gas-liquid separator. The device was designed by Dr. Paul Bommer with The University of Texas at Austin and is currently on file with the United States Patent and Trademark Office. A detailed description of the pump connector is provided. This includes a discussion of the theory underlying its design and possible applications for its use.

Two-phase annular flow occurs throughout this device. This flow has been well documented throughout the literature and is discussed in this report. Following this review are experimental results from testing performed at J.J. Pickle Research Campus at The University of Texas at Austin. Visual observation was used to characterize the upward gas-liquid flow in the prototype's concentric annulus. The pump connector exhibited flow regimes consistent with those seen in literature in its vertical orientation. Additional flow regime maps were generated at 10, 20 and 45 degrees. Increasing the inclination up to 45 degrees delayed the onset of churn flow and appeared to improve the effectiveness of this device. This is the first study to investigate fluid flow in this apparatus. The results of this

research will aid in a better understanding of the pump connector and assist in its improved design.

Table of Contents

List of Tables ix

List of Figures x

Chapter 1: Introduction 1

Chapter 2: Pump Connector 2

2.1: Theory 2

2.1.1: Down-Hole Gas Separators 2

2.1.2: Pump Discharge Pressure 5

2.1.2.1: Beam Lift 5

2.1.2.2: Electric Submersible Pumps 6

2.1.2.3: Gas Lift 7

2.1.2.4: Hydraulic Pumps 9

2.1.2.5: Progressing Cavity Pumps 10

2.2: Design 10

2.3: Applications 12

Chapter 3: Two-Phase Annular Flow 16

3.1: Flow Regime Classification 17

3.1.1: Bubble Flow 18

3.1.2: Slug Flow 18

3.1.3: Churn Flow 19

3.1.4: Annular Flow 19

3.2: Effect of Orientation 20

3.3: Flow Regime Maps 21

Chapter 4: Testing 25

4.1: Experimental Setup 25

4.2: Experimental Results 28

4.2.1: Flow Regime Characterization in Large Pump Connector 29

4.2.1.1: 0 Degrees (Vertical) 29

4.2.1.2: 10 Degrees 31
4.2.1.3: 20 Degrees 33
4.2.1.4: 45 Degrees 35
4.2.2: Flow Regime Characterization in Small Pump Connector 37
4.2.2.1: 0 Degrees (Vertical) 37
4.3: Discussion 38
Chapter 5: Conclusion 40
Nomenclature 41
References 42

List of Tables

Table 2.1: Liquid Capacity Example 5

Table 2.2: Pump Connector Dimensions (Bommer & University of Texas at Austin, 2014) 12

Table 4.1: Prototype Specifications 25

Table 4.2: Experimental Data for Large Pump Connector (0°) 29

Table 4.3: Experimental Data for Large Pump Connector (10°) 31

Table 4.4: Experimental Data for Large Pump Connector (20°) 33

Table 4.5: Experimental Data for Large Pump Connector (45°) 35

List of Figures

Figure 2.1: Down-Hole Gas-Liquid Separator (Bommer & Podio, 2012) 3

Figure 2.2: Beam Lift (Economides, Hill, & Ehlig-Economides, 1994) 6

Figure 2.3: Electric Submersible Pump (Cholet, 2008) 7

Figure 2.4: Gas Lift (Winkler & Blann, 2007) 8

Figure 2.5: Hydraulic Pumps (Lea, 2007) 9

Figure 2.6: Progressing Cavity Pump (Matthews, Zahacy, Alhanati, Skoczylas, & Dunn, 1997) 10

Figure 2.7: Pump Connector Design (Bommer & University of Texas at Austin, 2014) 11

Figure 2.8: Pump Connector Application (Bommer & University of Texas at Austin, 2014) 13

Figure 3.1: Laminar vs. Turbulent Flow (Bird, Stewart, & Lightfoot, 2002).....17

Figure 3.2: Flow Patterns in Vertical Flow (Kelessidis & Dukler, 1989) 18

Figure 3.3: Flow Patterns in Horizontal Flow (Hewitt & Hall-Taylor, 1970).....20

Figure 3.4: Bubble Flow Using PDF Analysis (Kelessidis & Dukler, 1989).....22

Figure 4.1: Pump Connector Prototypes.....26

Figure 4.2: Pump Connector Schematic 27

Figure 4.3: Pump Connector Experimental Setup 28

Figure 4.4: Experimental Pictures for Large Pump Connector (0°) 30

Figure 4.5: Comparison with Literature for Large Pump Connector (0°) 31

Figure 4.6: Experimental Pictures for Large Pump Connector (10°) 32

Figure 4.7: Flow Regime Map for Large Pump Connector (10°).....33

Figure 4.8: Experimental Pictures for Large Pump Connector (20°) 34

Figure 4.9: Flow Regime Map for Large Pump Connector (20°).....35
Figure 4.10: Experimental Pictures for Large Pump Connector (45°) 36
Figure 4.11: Flow Regime Map for Large Pump Connector (45°).....37

Chapter 1: Introduction

Two common problems facing pump assisted wells are the down-hole separation of gas from liquid and creating enough discharge pressure to flow fluids to the surface. One possible solution is a pump connector that doubles as a down-hole gas-liquid separator. This invention was proposed by Dr. Paul Bommer in conjunction with The University of Texas at Austin and is currently on file with the United States Patent and Trademark Office. Initial testing has begun on two different prototypes that were built in the University's machine shop.

The influx of fluid into the pump connector creates two-phase flow in a concentric annulus. The objective of this research was to better understand this flow, which could lead to improvements in the equipment's design. This was accomplished by performing a literature review of two-phase annular flow and relating these findings to experimental observations of flow in the actual apparatus.

This report would be remiss without a thorough description of the design and application of the pump connector itself, so it will begin there. It will then proceed to a comprehensive literature review of two-phase annular flow, followed by a chapter on the study's experimental procedures and results. It will conclude by summarizing all findings, discussing their significance and providing recommendations for future authors interested in the design and application of this device.

Chapter 2: Pump Connector

The pump connector is intended to facilitate the down-hole separation of gas from liquid and boost discharge pressure. This chapter will begin with a discussion of these topics. A proper understanding of the theory will assist in the comprehension of the device's application and design.

2.1: THEORY

2.1.1: Down-Hole Gas Separators

Pumps are designed for liquid, not gas. The influx of gas can hinder performance and reduce pump life. This is especially problematic in pump assisted oil wells, because gas is commonly co-produced with liquids. Gas can be solution gas or free gas. Whatever its form, it is advantageous to keep gas from entering the pump. This is the goal of down-hole gas separators.

Figure 1 is a schematic of a down-hole gas-liquid separator reproduced from *The Beam Lift Handbook* (Bommer & Podio, 2012). In the figure, fluids are being produced from the perforations below the pump intake. This permits gas to enter the pump. This issue could be resolved by placing the pump intake below the perforations, however this is not always possible. In a horizontal well, the pump is often placed in the vertical section but is produced from the horizontal section. This situation would benefit from a down-hole separator.

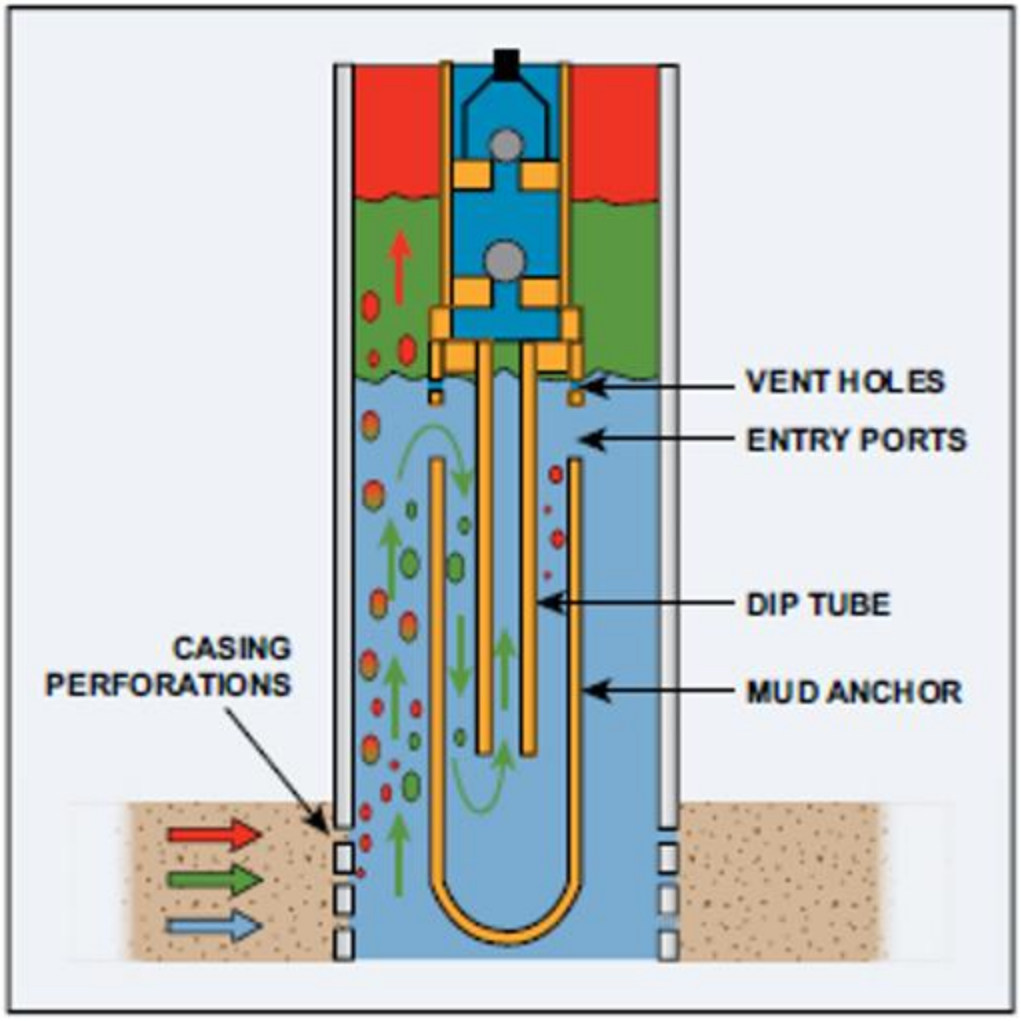

Figure 2.1: Down-Hole Gas-Liquid Separator (Bommer & Podio, 2012)

The down-hole separator consists of a mud anchor, dip tube, entry ports and vent holes. The combination of dip tube and mud anchor creates a weir. Gas can still flow up the casing-tubing annulus, as before, but fluid entering the pump must flow through the entry ports, over the weir and through the dip tube-mud anchor annulus. This fluid contains entrained gas, which has an upward velocity relative to its liquid counterpart. This is defined as gas bubble slip velocity and depends on bubble size and gas and liquid properties (Bommer & Podio, 2012). When the gas bubble slip velocity exceeds the downward fluid

velocity, the gas rises and escapes through the vent holes to be produced with the rest of the gas through the casing-tubing annulus.

It is not practical to design a separator to remove all gas. As bubble size decreases, gas bubble slip velocity can decrease to a few inches per second (Bommer & Podio, 2012). To maintain adequate separation, liquid velocity is decreased by reducing production at surface. This is not economical, so operators define a minimum bubble size to be separated. A ¼ inch diameter is routinely chosen, which has a gas bubble slip velocity of 6 inches per second (Bommer & Podio, 2012).

Down-hole gas separators are designed and operated so that the desired liquid velocity does not exceed this critical threshold. The maximum rate is defined as liquid capacity and is calculated as follows:

$$q_l = 42.0(ID_{ma}^2 - OD_{dt}^2) \quad \text{(2.1)}$$

Where:

$q_l = liquid\ capacity\ (bpd)$

$ID_{ma} = internal\ diameter\ of\ mud\ anchor\ (in)$

$OD_{dt} = outer\ diameter\ of\ dip\ tube\ (in)$

For example, the liquid capacity of a separator with specifications in Table 2.1 is 25.6 barrels per day. This is 6 inches per second down-hole and will separate gas bubbles ¼ inch and greater.

Table 2.1: Liquid Capacity Example

Mud Anchor		Dip Tube		Liquid Capacity
OD (in)	ID (in)	OD (in)	ID (in)	(bbl/day)
2.75	2.5	2.375	2	25.6

By producing at or below this limit, operators can prevent most gas from entering the pump. This improves performance, prolongs life and makes down-hole pumps an attractive option in lifting stagnant fluids to the surface.

There will be situations when the reservoir rate exceeds the liquid capacity of the separator. This will cause the separator to fail and reduce the volumetric efficiency of the pump. Operators must use discretion when implementing this technology.

2.1.2: Pump Discharge Pressure

Reservoir pressure is a key factor that determines whether a fluid will rise to the surface. If reservoir pressure exceeds the hydrostatic head of the overriding fluid column and pipe friction, fluids can be produced without assistance. As production ensues, reservoir pressure declines and the well may no longer flow.

Pumps can provide the additional pressure needed to bring fluids to the surface. This added pressure is defined as discharge pressure and is the pressure of the fluid exiting the pump. The pump connector can link two pumping technologies together and increase discharge pressure. Discharge pressure can mean different things in different contexts. A discussion of the various artificial lift technologies is therefore warranted.

2.1.2.1: Beam Lift

Beam lift uses the mechanical motion of a plunger to lift fluids to the surface. In Figure 2.2, the tubing string is filled with reservoir fluid. The pressure at the bottom of the

tubing, just above the pump, is the pump discharge pressure. The pump must compress the fluid to a pressure greater than this for fluid to enter the pump and be lifted to the surface.

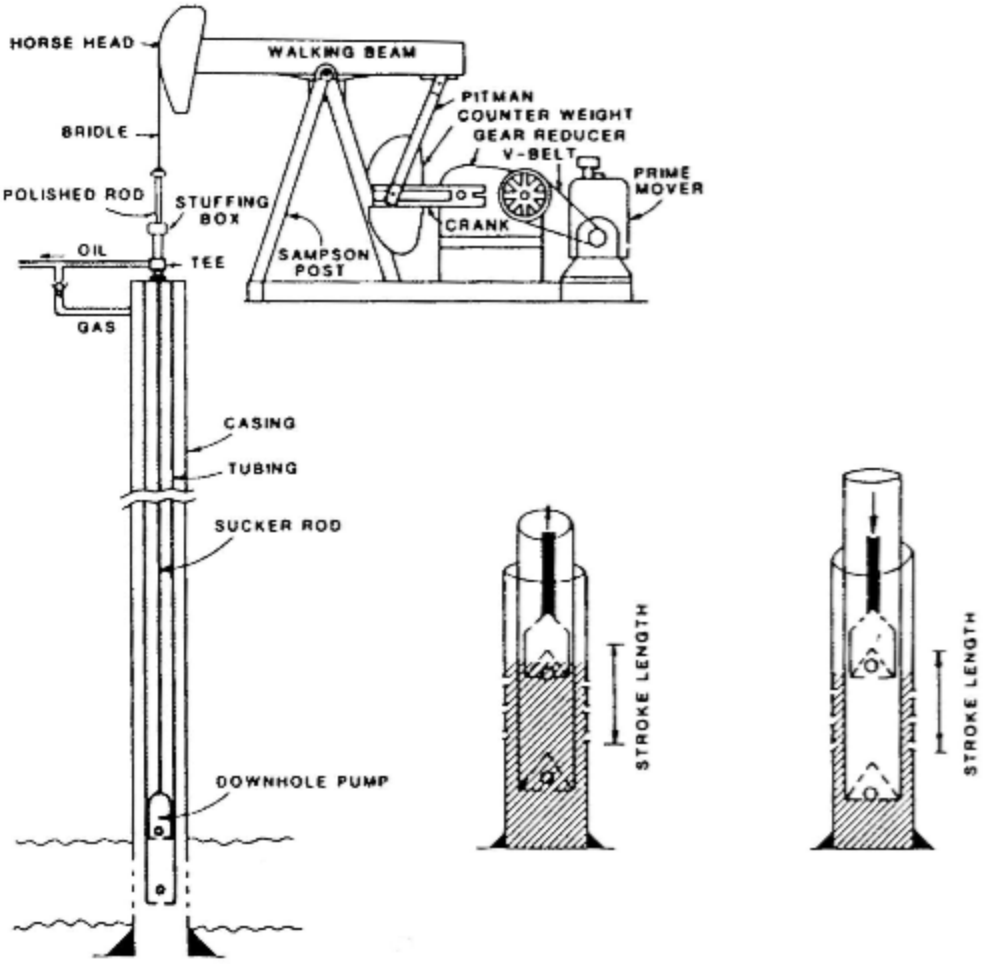

Figure 2.2: Beam Lift (Economides, Hill, & Ehlig-Economides, 1994)

2.1.2.2: Electric Submersible Pumps

An electric submersible pump (ESP) is a multistage centrifugal pump. A typical configuration consists of tubing hung from the wellhead with the pump on top and the motor attached below. Pump discharge pressure is created by the kinetic energy change of

the fluid as it passes through each pump stage. It eventually becomes the pressure of the fluid exiting the pump.

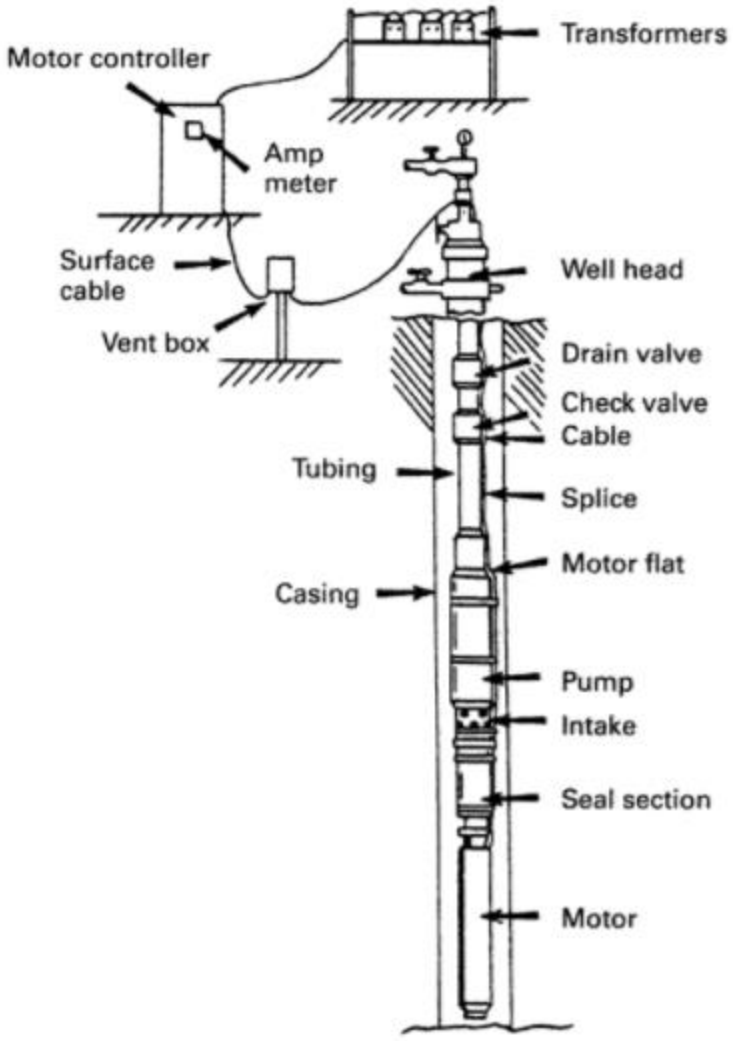

Figure 2.3: Electric Submersible Pump (Cholet, 2008)

2.1.2.3: Gas Lift

Gas lift uses injected gas to decrease the density of the wellbore fluid. This decreases the hydrostatic head above the formation fluid, which allows the remaining

reservoir pressure to drive liquids to the surface. Pump discharge pressure is a term not often used with gas lift. This is because gas lift does not utilize a down-hole pump. However, gas lift can be used in conjunction with the pump connector. In this context, the pump discharge pressure is the difference between the gasified wellbore fluid and the reservoir fluid.

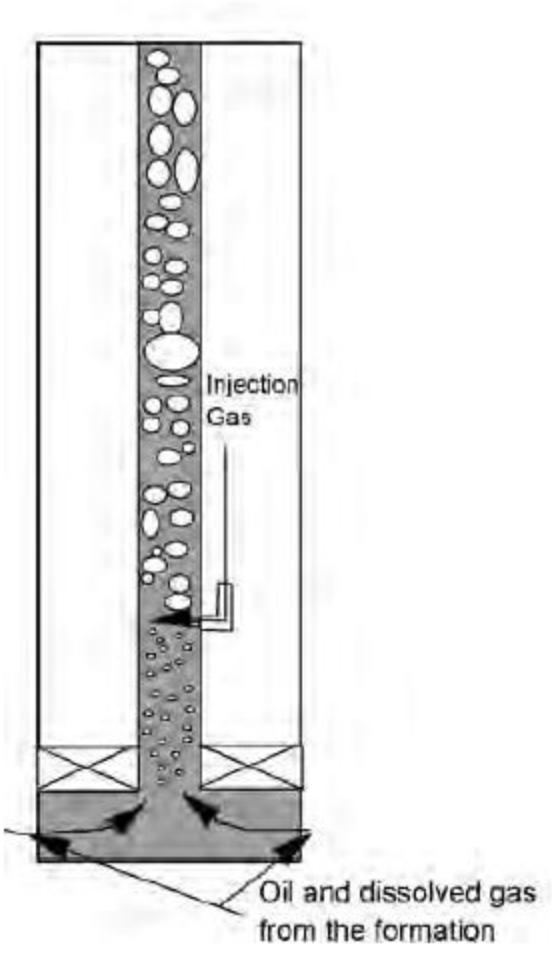

Figure 2.4: Gas Lift (Winkler & Blann, 2007)

2.1.2.4: Hydraulic Pumps

Hydraulic pumps inject fluid from the surface to increase the pressure of the reservoir fluid. The injected fluid is called power fluid and is typically oil or produced water (Lea, 2007). A positive displacement pump (left) is one example of a hydraulic pump. These pumps have pistons that transfer energy from the power fluid to the reservoir fluid. Jet pumps (right) are another example. In jet pumps, the power fluid passes through a nozzle and mixes with the reservoir fluid. The mixture then passes through a Venturi throat and diffuser, which increases fluid pressure by a change in kinetic energy. In both applications, the pump discharge pressure is the pressure of the fluid exiting the pump.

a) Positive Displacement Pump

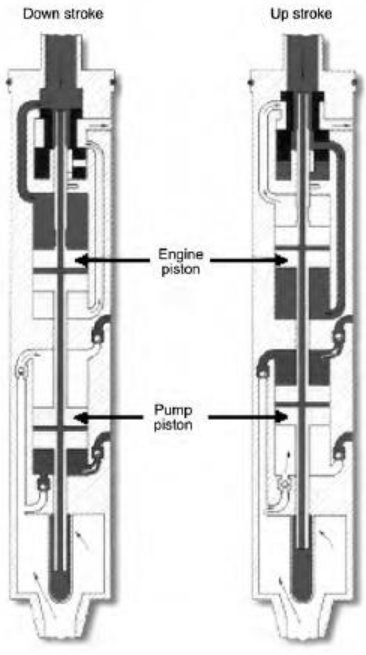

b) Jet Pump

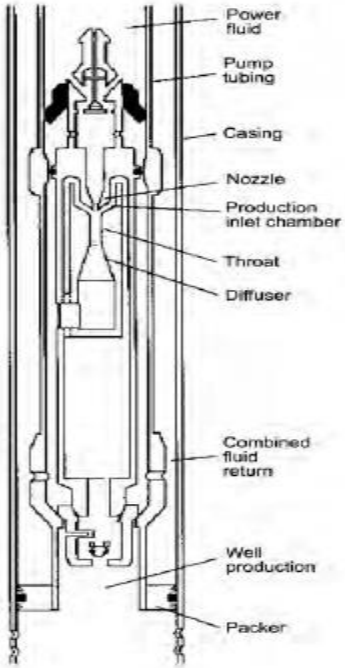

Figure 2.5: Hydraulic Pumps (Lea, 2007)

2.1.2.5: Progressing Cavity Pumps

A progressing cavity pump is a positive displacement pump. A rotor displaces formation fluids one cavity at a time like a plunger pump. The pump is designed so that fluids exit the pump with enough pressure to flow to the surface. This is the pump discharge pressure.

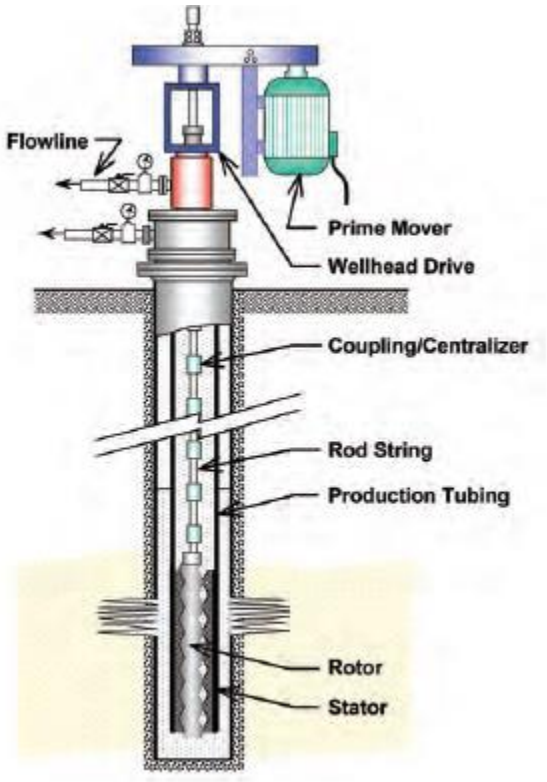

Figure 2.6: Progressing Cavity Pump (Matthews, Zahacy, Alhanati, Skoczylas, & Dunn, 1997)

2.2: DESIGN

Figure 2.8 is a schematic of the pump connector that was submitted to United States Patent and Trademark Office. Fluid enters the bottom of the pump connector from another pump or the wellbore if no other pump is attached. The fluid then passes through an optional foam breaker as it fills up the outside tube. As the outside tube fills, fluid travels

into the middle tube as if flowing over a weir. This is the fall back tube for liquid feed to the top pump. Beam lift is used in this example, but any pump would suffice. Fluid then enters the beam pump through the inside tube and is lifted to the surface. Excess fluid that does not enter the fall back tube overflows to the bottom of the well where it can reenter the pump connector.

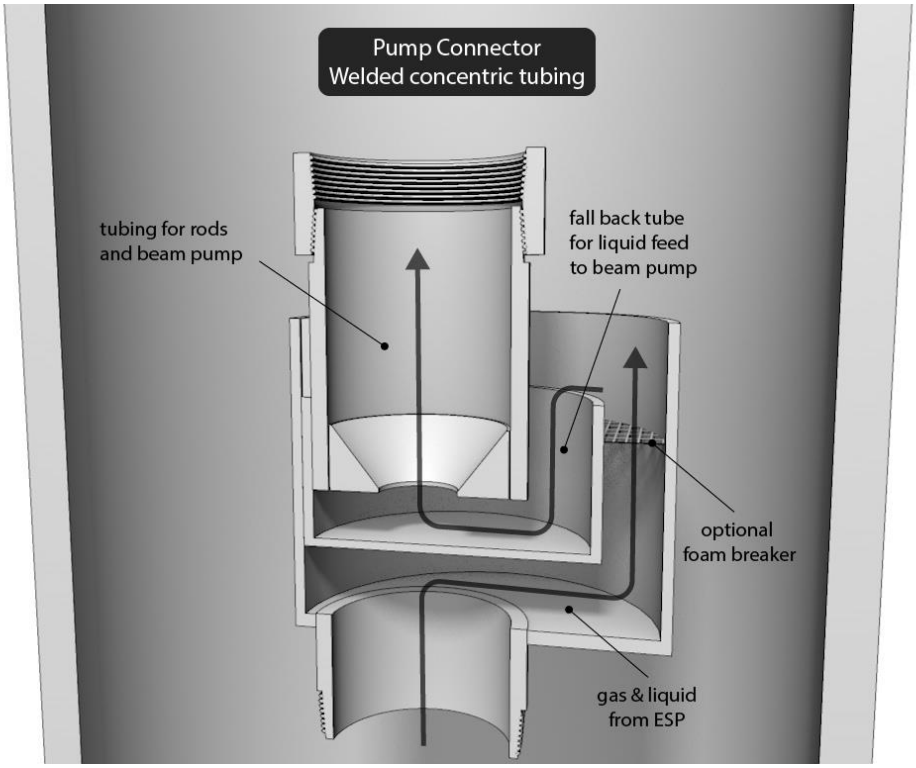

Figure 2.7: Pump Connector Design (Bommer & University of Texas at Austin, 2014)

The pump connector is designed so that the outside tube has the maximum possible diameter. Since the outside tube must fit within the casing, the casing string's inside diameter is the limiting constraint. The size of the outside tube determines the size of the middle tube, which is also designed to be as large as possible while still permitting flow. The inside tube has dimensions consistent with standard production tubing.

The length of the connector is determined by the output of the beam pump. A longer length is desired, because it creates a larger reservoir of fluid in the fall back tube. This increases the likelihood that that there will be liquid feed for the beam pump. A convenient length is 33 feet, which is the length of a standard joint of tubing. Table 2.2 lists the recommended dimensions for different sizes of casing.

Table 2.2: Pump Connector Dimensions (Bommer & University of Texas at Austin, 2014)

Casing	Outside Tube			Middle Tube			Inside Tube	
OD (in)	OD (in)	ID (in)	Length (ft)	OD (in)	ID (in)	Length (ft)	OD (in)	ID (in)
4.5/11.6	3.5	3	32	2.75	2.5	29	2.375	2
5.5/17 ppf	4.5	4	32	3.5	3.25	29	2.375	2
7/29 ppf	5.5	4.95	32	4.5	4	29	2.875	2.441

2.3: APPLICATIONS

The pump connector can replace a traditional down-hole gas separator. In the latter, fluid entering the pump must flow through the entry ports, over the weir and through the dip tube-mud anchor annulus. This is like the connector, where fluid flows over the weir and through the middle tube-inside tube annulus. Since the designs are similar, the connector is also expected to separate gas bubbles ¼ inch and greater if incoming liquid rate is kept below 6 inches per second. The difference between the two devices is that the connector requires a packer or lower pump to force fluids into its inlet.

The pump connector can also increase discharge pressure by linking two pumps together. This is advantageous in deep wells where a single pump is not sufficient to lift fluids to the surface. In Figure 2.9, the reservoir does not have enough energy to lift fluids to the beam pump, so it is connected to an electric submersible pump. The pump intake of

the ESP is placed at the well's deepest point, which maximizes reservoir drawdown. Fluids are lifted until the ESP's discharge pressure is completely exhausted. The fluid then passes through the pump connector, where gas is separated, and to the beam pump where it is lifted to the surface. Any overflow fluid falls back to the bottom of the well to be reprocessed by the ESP.

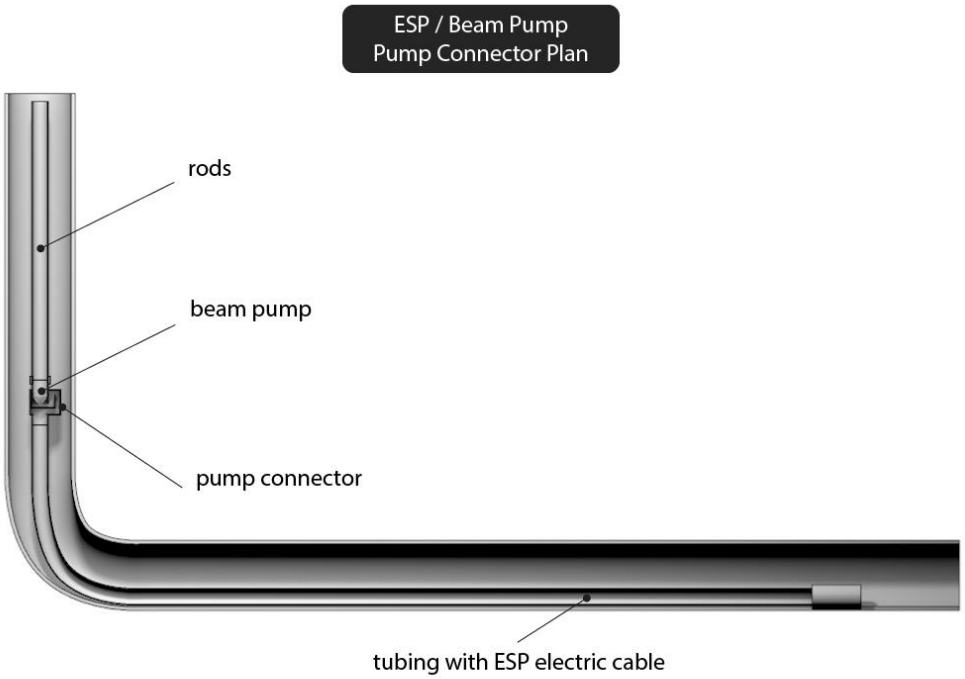

Figure 2.8: Pump Connector Application (Bommer & University of Texas at Austin, 2014)

This configuration is advantageous for several reasons. Beam pumps are ineffective in deviated wells. Since the reservoir pressure has declined, the maximum rate of formation fluids cannot reach the intake of the beam pump in the vertical section of the well. The

pump connector resolves this issue by linking the beam pump to an ESP to reach the formation fluids.

For smaller flow rates, a large ESP could be used by itself, but the device would have to create enough discharge pressure to flow fluids to the surface. This would cause heat dissipation issues resulting in a short pump life and is not economical if only a small volume of fluid is to be lifted.

Finally, since an ESP also uses a gas-liquid separator, the fluid reaching the pump connector has already been pre-processed to remove gas. As fluid flows through the connector, additional gas is removed. By linking two pumps together, the connector has also linked two separators together. This reduces the gas-liquid ratio of the fluid entering the top pump or enables the production of fluids with higher gas-liquid ratios to begin with. The former can improve the life and performance of the surface pump. Altogether, the pump connector enables the production of fluids that had previously been impractical to recover.

The connector will work with multiple combinations of pumps, including: beam lift; electric submersible pumps; hydraulic pumps; and progressing cavity pumps. In each case, the bottom pump should contact reservoir fluids at its intake and transfer the fluids to the pump connector when its discharge pressure is depleted. The top pump should have enough discharge pressure to then lift fluids to the surface.

The bottom pump can also be replaced with a tubing string to inject gas. Gas lift can raise the fluids to the pump connector where a different pump takes over. This is a substitute for gas lift in low bottom hole pressure wells.

Finally, the connector can also be used without a bottom pump. In this way, it replaces a traditional down-hole gas separator. This could be of commercial interest depending on how cheaply the connector can be made.

As this chapter described, the pump connector has many potentially useful applications. One possible issue that may affect its performance is the annular flow between its middle and outside tubes. An investigation of two-phase annular flow regimes is therefore needed. A background of this theory is discussed in the next chapter.

Chapter 3: Two-Phase Annular Flow

The same fluid can display different behavior in dissimilar conditions. Consider the simple case of single-phase flow through a horizontal tube. For Reynolds number less than 2100, flow is laminar. Its fluid layers move smoothly over one another in the direction of flow. Reynolds number is the ratio of inertial to viscous forces:

$$Re = \frac{\rho u L}{\mu} = \frac{u L}{v} \quad \text{..... (3.1)}$$

Where:

$Re = Reynolds\ number$

$\rho = density\ of\ the\ fluid$

$u = velocity\ of\ the\ fluid\ with\ respect\ to\ the\ object$

$L = characteristic\ linear\ dimension$

$\mu = dynamic\ viscosity\ of\ the\ fluid$

$v = kinematic\ viscosity\ of\ the\ fluid$

If conditions change and the Reynolds number exceeds 2100, flow becomes turbulent. Turbulent flow is a complex flow pattern characterized by motion perpendicular to the principal flow direction. Figure 3.1 illustrates this difference. The top flow is laminar, while the bottom flow is turbulent.

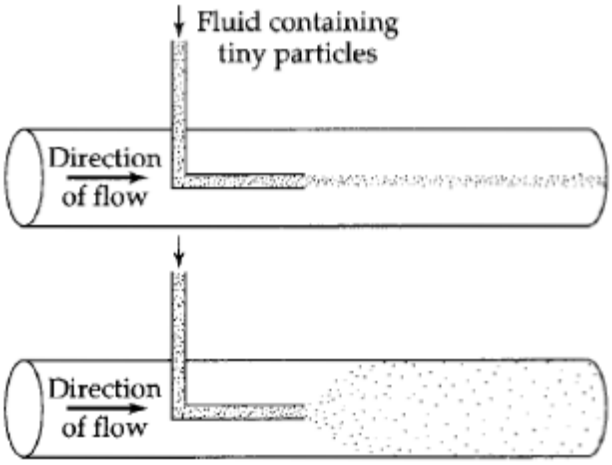

a) Laminar Flow

b) Turbulent Flow

Figure 3.1: Laminar vs. Turbulent Flow (Bird, Stewart, & Lightfoot, 2002)

Additional flow patterns emerge for the two-phase flow of liquid and gas and when the fluid is directed through an annulus. The resulting flow regimes are discussed in the following section.

3.1: Flow Regime Classification

Upward two-phase flow in a vertical concentric annulus can be classified into four basic flow patterns. This is illustrated in Figure 3.2. The flow regimes consist of: bubble flow; slug flow; churn flow; and annular flow. The characteristics of each flow regime are discussed next.

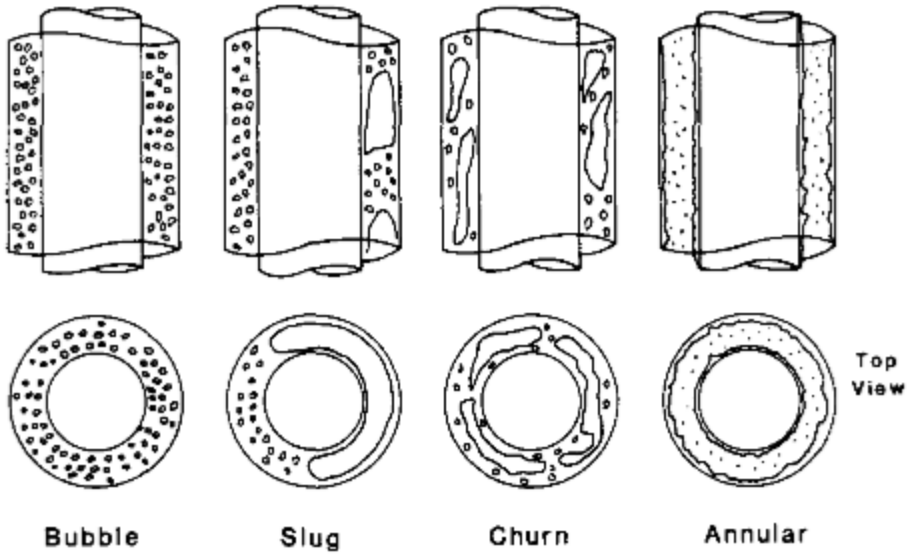

Figure 3.2: Flow Patterns in Vertical Flow (Kelessidis & Dukler, 1989)

3.1.1: Bubble Flow

Bubble flow displays discrete gas bubbles dispersed throughout the continuous liquid phase.

3.1.2: Slug Flow

In slug flow, the gas bubbles begin to coalesce to form Taylor bubbles. Taylor bubbles are large bubbles of the lighter phase that form by coalescence of small bubbles under certain flow conditions (Davies & Taylor, 1950). Most gas flow occurs in the Taylor bubbles. The bubbles are wrapped around the inside tube with liquid falling downwards in the space between the Taylor bubbles and the walls of the annulus. In between the Taylor bubbles are liquid slugs, which contain gas bubbles that have not yet coalesced.

Taylor bubbles can appear when the average annulus perimeter is lower than the distorted bubble limit (Hernández, Julia, Ozar, Hibiki, & Ishii, 2011). Distorted bubbles

are another class of bubbles that precede the formation of Taylor bubbles (Ishii & Hibiki, 2011). The average annulus perimeter and distorted bubble limit are defined as follows:

$$P_{ave} = \pi * \frac{D_i + D_o}{2} \quad \text{(3.2)}$$

$$D_{d,max} = 4 * \sqrt{\frac{\sigma}{g * \Delta\rho}} \quad \text{(3.3)}$$

Where:

$P_{ave} = average\ annulus\ perimeter$

$D_i = inner\ annulus\ diameter$

$D_o = outer\ annulus\ diameter$

$D_{d,max} = maximum\ distorted\ bubble\ limit$

$\sigma = surface\ tension$

$g = gravitational\ acceleration$

$\Delta\rho = density\ difference\ between\ two\ phases$

3.1.3: Churn Flow

Churn flow is like slug flow but more chaotic. In churn flow, the gas lifts the liquid as it moves throughout the annulus. At a certain point, the liquid falls, collects and forms a bridge around the inside tube. The process repeats itself in an oscillatory motion as the gas re-lifts the accumulated liquid.

3.1.4: Annular Flow

Annular flow occurs when the liquid phase flows along the walls as a film and the gas flows in the center. The gas may also contain some entrained liquid. At very high flow rates, these droplets can agglomerate and coalesce forming a frothy two-phase mixture.

This is a special case and is referred to as annular flow with lumps (Kelessidis & Dukler, 1989).

3.2: Effect of Orientation

The orientation of the annulus can also influence the flow pattern. The vertical case was discussed in detail, because this is the pump connector's intended state. However, a complete subset of flow regimes exists for the horizontal case. These include: bubbly flow; plug flow; stratified flow; wavy flow; slug flow; and annular flow. These patterns are reproduced in Figure 3.3 below:

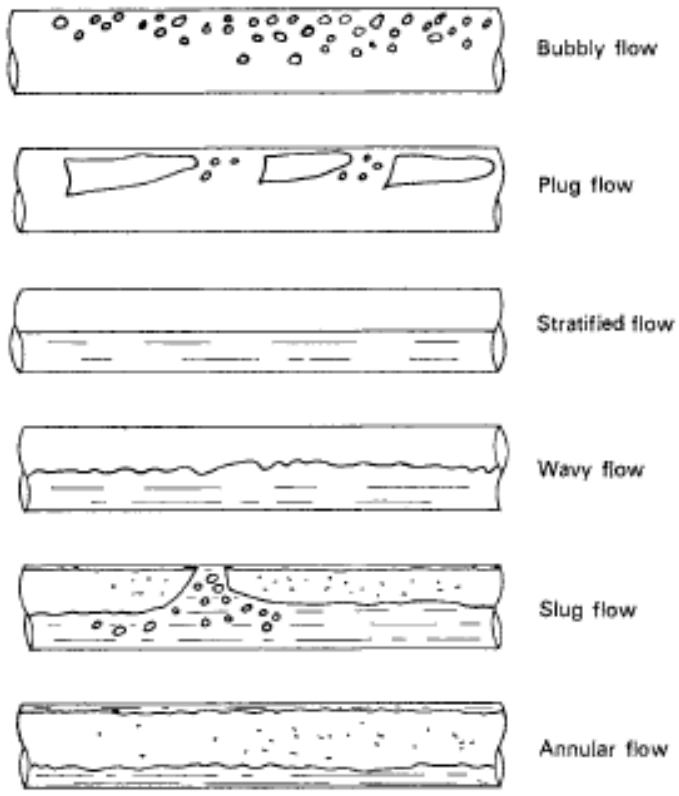

Figure 3.3: Flow Patterns in Horizontal Flow (Hewitt & Hall-Taylor, 1970)

Situations may exist when the pump connector deviates from the vertical. An inclined annulus exhibits flow patterns that lie between the vertical and horizontal regimes (Hewitt & Hall-Taylor, 1970). This effect was studied and will be discussed in the following chapter.

3.3: Flow Regime Maps

A flow regime map is a tool to illustrate the transition between flow patterns. The map is constructed by observing how the flow regime changes with varying conditions. Gas and liquid rates are adjusted while the fluid properties and annular geometry remain constant. The simplest way to identify the resulting fluid flow regime is through visual observation, although this method is highly subjective. A more robust technique is to use conductivity probes to distinguish between the gas and liquid phases. In this method, the probes contact the two-phase mixture and exhibit a time-varying voltage drop as current flows through them. If the mixture is mostly liquid, the voltage drop is large. If the mixture is mostly gas, the voltage drop is small. This information is then used to classify the specific regime. A variety of statistical and machine learning techniques are used for this step. In Kelessidis and Dukler (1989), classification was achieved using probability density function analysis.

Each flow regime exhibits a specific voltage fingerprint. In bubble flow, the probe will contact mostly liquid and its PDF plot will show a distribution with a single peak near the maximum voltage values. This is shown in Figure 3.4:

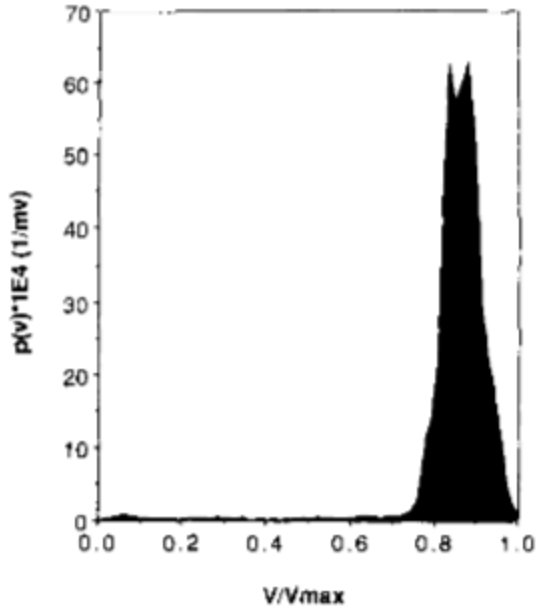

Figure 3.4: Bubble Flow Using PDF Analysis (Kelessidis & Dukler, 1989)

This statement can also be expressed mathematically as:

$$A\ single\ peak\ exists\ at\ {}^{V}/_{V_{max}}\ near\ 1.0\ such\ that\ \int \rho dv = 1\ for\ {}^{V}/_{V_{max}} > 0.75 \quad \text{..... (3.4)}$$

Where:

$V = measured\ voltage$

$V_{max} = maximux\ voltage\ for\ which\ a\ non-zero\ PDF\ value\ is\ estimated$

Each flow regime can be uniquely described in this way. Using these criteria, a flow regime map can be constructed by recording data over a range of superficial gas and liquid velocities:

$$U_{GS} = \epsilon U_G \quad \text{(3.5)}$$

$$U_{LS} = (1 - \epsilon) U_L \quad \text{(3.6)}$$

Where:

$U_{GS} = superficial\ gas\ bubble\ velocity$

$\epsilon = void\ fraction$

$U_G = gas\ bubble\ velocity$

$U_{LS} = superficial\ average\ liquid\ velocity$

$U_L = average\ liquid\ velocity$

The results of this process are shown in Figure 3.5:

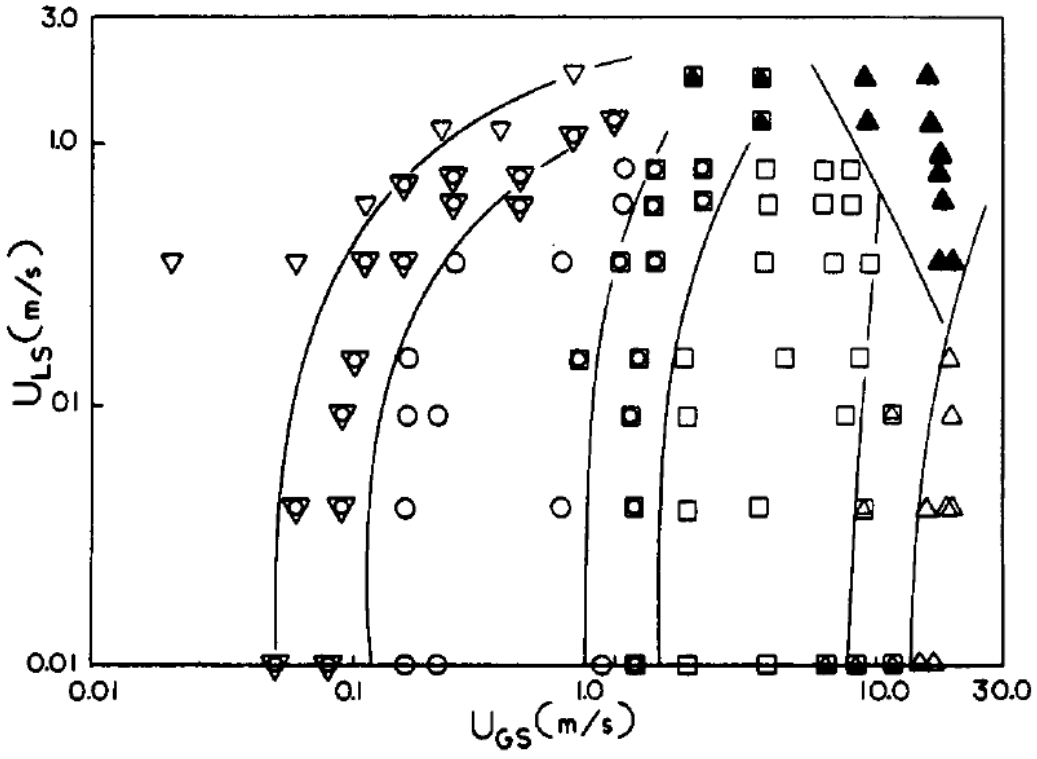

▽, Bubble flow; ○, slug flow; □, churn flow; △, annular flow; ▲, annular flow with lumps.

Figure 3.5: Flow Regime Map (Kelessidis & Dukler, 1989):

The symbols denote the flow pattern at a specific gas and liquid rate. Lines are drawn to display the transition between flow regimes. This figure was used as a template to identify the flow patterns in the pump connector annulus. The results of these experiments are discussed in the next chapter.

Chapter 4: Testing

This chapter will include a description of the experimental setup, followed by a discussion of all results. All testing was performed at J.J. Pickle Research Campus at The University of Texas at Austin.

4.1: Experimental Setup

Two prototypes were built with the following specifications:

Table 4.1: Prototype Specifications

Description	Outside Tube			Middle Tube			Inside Tube	
	OD (in)	ID (in)	Length (ft)	OD (in)	ID (in)	Length (ft)	OD (in)	ID (in)
Small	3.25	3	5	2.75	2.5	3	2.375	2.125
Large	6	5.5	6	4.5	4	4	3	2.5

Both designs consisted of acrylic tubing to permit visual observation of the resulting flow patterns. The devices are pictured in Figure 4.1 below:

Figure 4.1: Pump Connector Prototypes

In each test, liquid water and compressed air were injected into the bottom of the pump connector. The flow rates were recorded with liquid and gas meters. As fluids were injected, the outside tube-middle tube annulus began to fill. After reaching the height of the middle tube, the fluid flowed over the middle tube into the middle tube-inside tube annulus. The fluid then entered the inside tube through entry ports and a standing valve. The standing valve was added to prevent backflow. When these regions filled, the fluid resumed its rise in the outside tube-middle tube annulus until it eventually overflowed onto the ground. A plunger rod was used to lift the fluids out of the device through the inside

tube. This caused the fluid level in the outside tube-middle tube annulus to drop. The stroke rate of the plunger rod was manipulated by hand to keep the fluid level between the height of the outside and middle tubes. A schematic of the experimental setup is reproduced in Figure 4.2 with accompanying pictures in Figure 4.3:

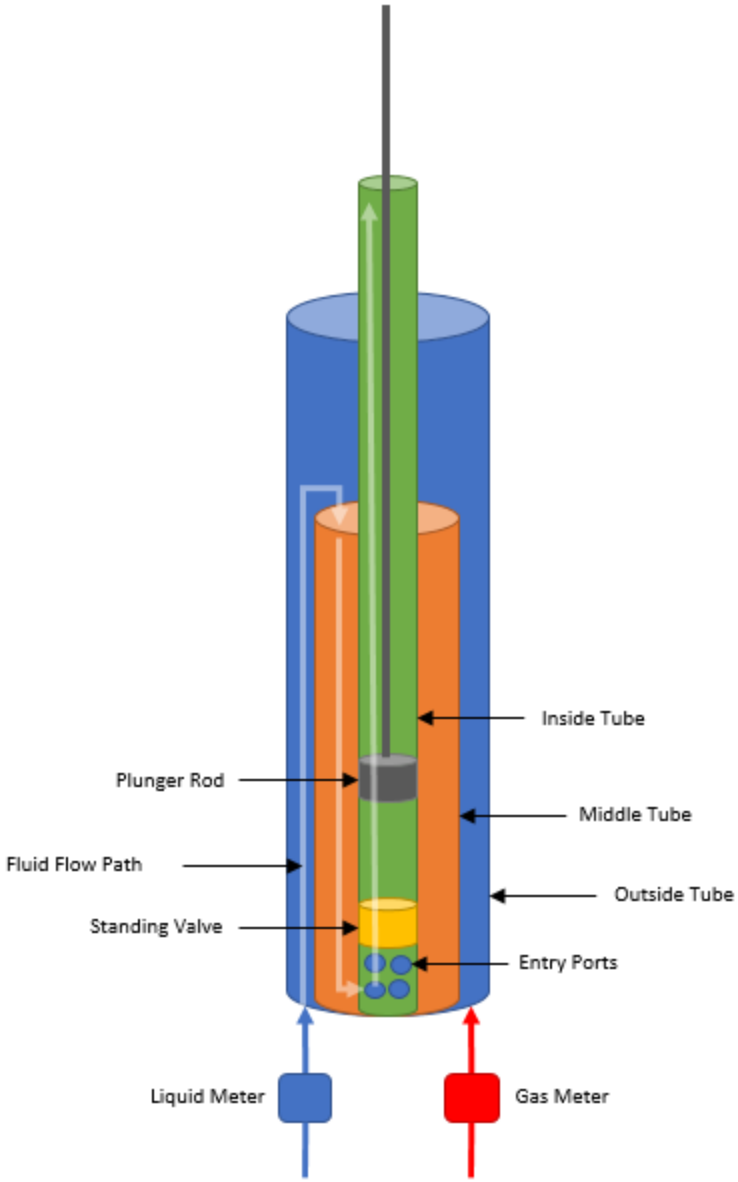

Figure 4.2: Pump Connector Schematic

Figure 4.3: Pump Connector Experimental Setup

4.2: Experimental Results

The flow regimes were characterized in each pump connector at a variety of conditions. The gas and liquid rates, as well as the orientation of the device, were systematically altered. The separating capabilities of the pump connectors were also tested, but will be discussed in Adi Suresh's forthcoming Spring 2018 thesis. The results of these experiments are discussed in the following subsections.

4.2.1: Flow Regime Characterization in Large Pump Connector

4.2.1.1: 0 Degrees (Vertical)

Table 4.2: Experimental Data for Large Pump Connector (0°)

Test	*Air Rate*	*Air Rate*	*Water Rate*	*Water Rate*	*Flow Regime*	*Flow Regime*
	lit/min	*m/s*	*gal/min*	*m/s*	*(Observed)*	*(Predicted)*
1	16	0.05	4.39	0.05	Bubble	Bubble
2	21	0.07	4.39	0.05	Bubble	Bubble
3	30	0.10	4.37	0.05	Bubble	Bubble
4	48	0.16	4.37	0.05	Bubble	Slug
5	197	0.65	4.37	0.05	Churn	Slug
6	457	1.50	4.41	0.05	Churn	Churn
7	465	1.53	10.22	0.13	Churn	Churn
8	520	1.71	8.7	0.11	Churn	Churn
9	12	0.04	8.73	0.11	Bubble	Bubble

Figure 4.4: Experimental Pictures for Large Pump Connector (0°)

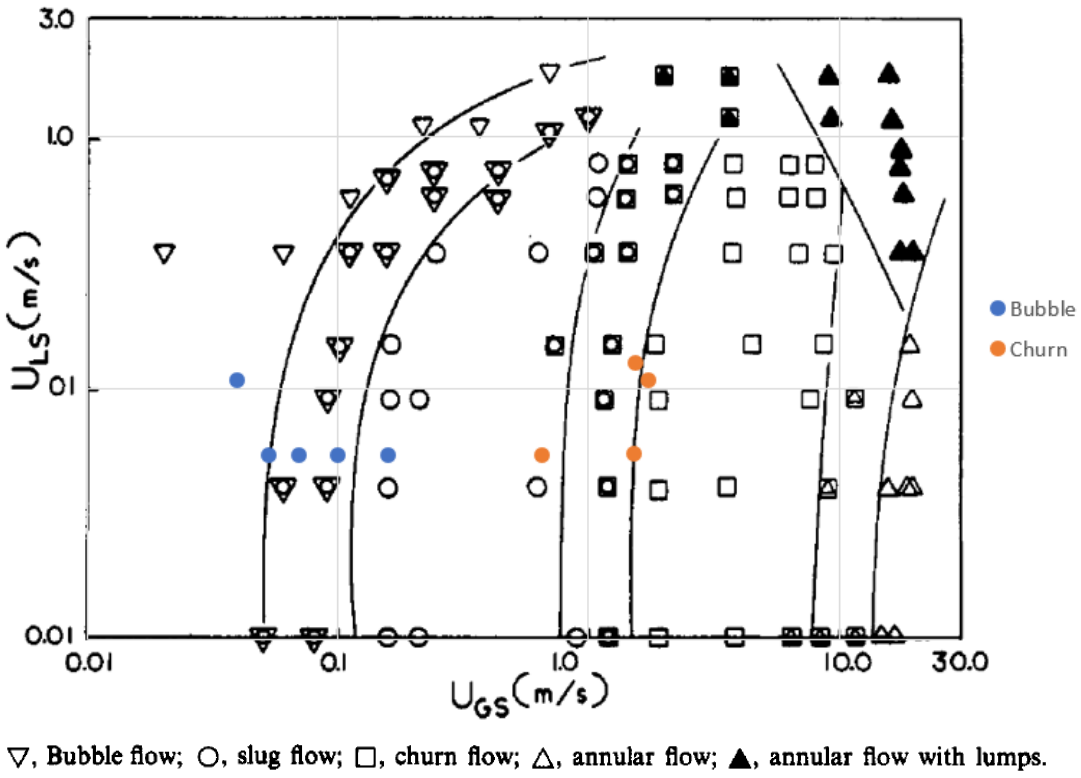

Figure 4.5: Comparison with Literature for Large Pump Connector (0°)

4.2.1.2: 10 Degrees

Table 4.3: Experimental Data for Large Pump Connector (10°)

Test	*Air Rate*	*Air Rate*	*Water Rate*	*Water Rate*	*Flow Regime*	*Flow Regime*
	lit/min	*m/s*	*gal/min*	*m/s*	*(Observed)*	*(Predicted)*
1	17	0.06	4.41	0.05	Bubble	-
2	21	0.07	4.41	0.05	Bubble	-
3	29	0.10	4.41	0.05	Bubble	-
4	48	0.16	4.41	0.05	Bubble	-
5	195	0.64	4.41	0.05	Churn	-
6	457	1.50	4.41	0.05	Churn	-
7	460	1.51	10.21	0.13	Churn	-
8	518	1.70	8.71	0.11	Churn	-
9	19	0.06	8.69	0.11	Bubble	-

Figure 4.6: Experimental Pictures for Large Pump Connector (10°)

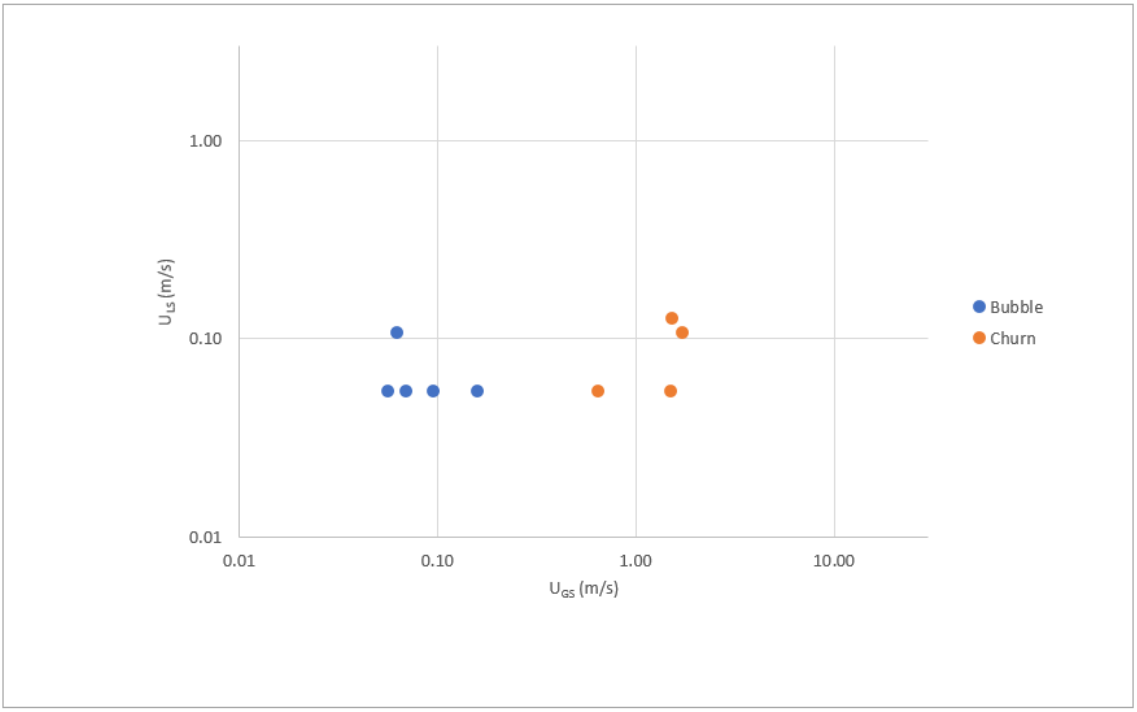

Figure 4.7: Flow Regime Map for Large Pump Connector (10°)

4.2.1.3: 20 Degrees

Table 4.4: Experimental Data for Large Pump Connector (20°)

Test	*Air Rate*	*Air Rate*	*Water Rate*	*Water Rate*	*Flow Regime*	*Flow Regime*
	lit/min	*m/s*	*gal/min*	*m/s*	*(Observed)*	*(Predicted)*
1	14	0.05	4.41	0.05	Bubble	-
2	20	0.07	4.41	0.05	Bubble	-
3	30	0.10	4.41	0.05	Bubble	-
4	55	0.18	4.41	0.05	Bubble	-
5	189	0.62	4.41	0.05	Bubble	-
6	460	1.51	4.41	0.05	Churn	-
7	455	1.50	10.21	0.13	Churn	-
8	520	1.71	8.71	0.11	Churn	-
9	15	0.05	8.75	0.11	Bubble	-

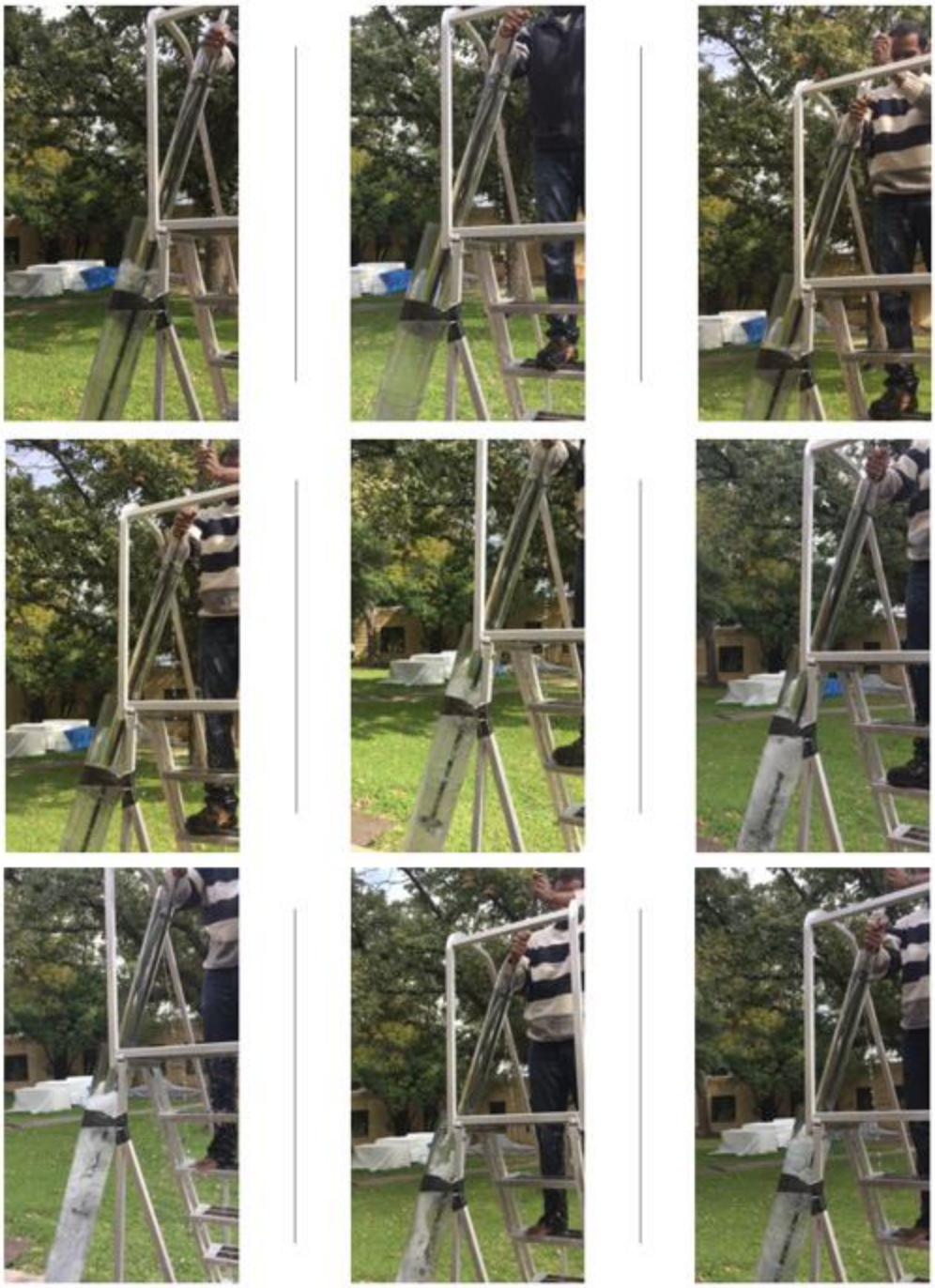

Figure 4.8: Experimental Pictures for Large Pump Connector (20°)

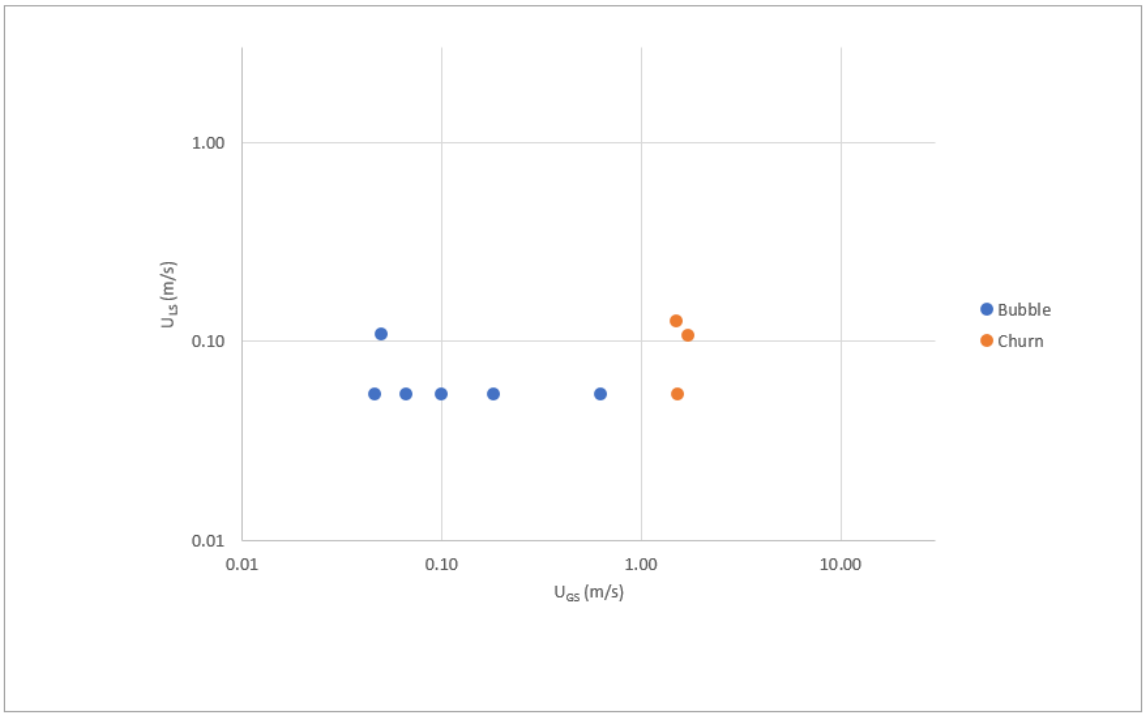

Figure 4.9: Flow Regime Map for Large Pump Connector (20°)

4.2.1.4: 45 Degrees

Table 4.5: Experimental Data for Large Pump Connector (45°)

Test	*Air Rate*	*Air Rate*	*Water Rate*	*Water Rate*	*Flow Regime*	*Flow Regime*
	lit/min	*m/s*	*gal/min*	*m/s*	*(Observed)*	*(Predicted)*
1	15	0.05	4.43	0.06	Bubble	-
2	20	0.07	4.43	0.06	Bubble	-
3	29	0.10	4.43	0.06	Plug	-
4	45	0.15	4.43	0.06	Plug	-
5	197	0.65	4.43	0.06	Slug	-
6	455	1.50	4.43	0.06	Churn	-
7	457	1.50	10.21	0.13	Churn	-
8	520	1.71	8.66	0.11	Churn	-
9	22	0.07	8.84	0.11	Bubble	-

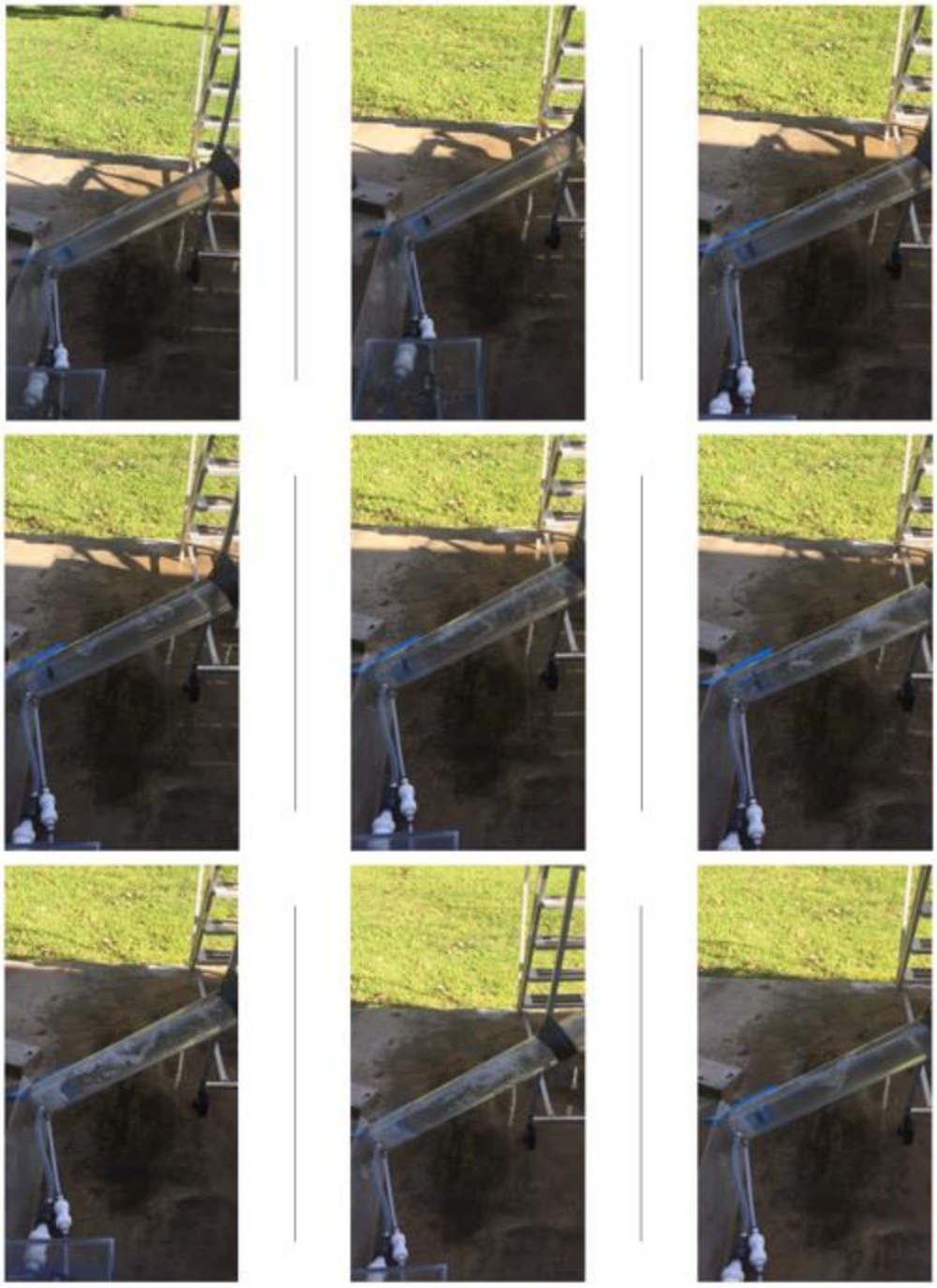

Figure 4.10: Experimental Pictures for Large Pump Connector (45°)

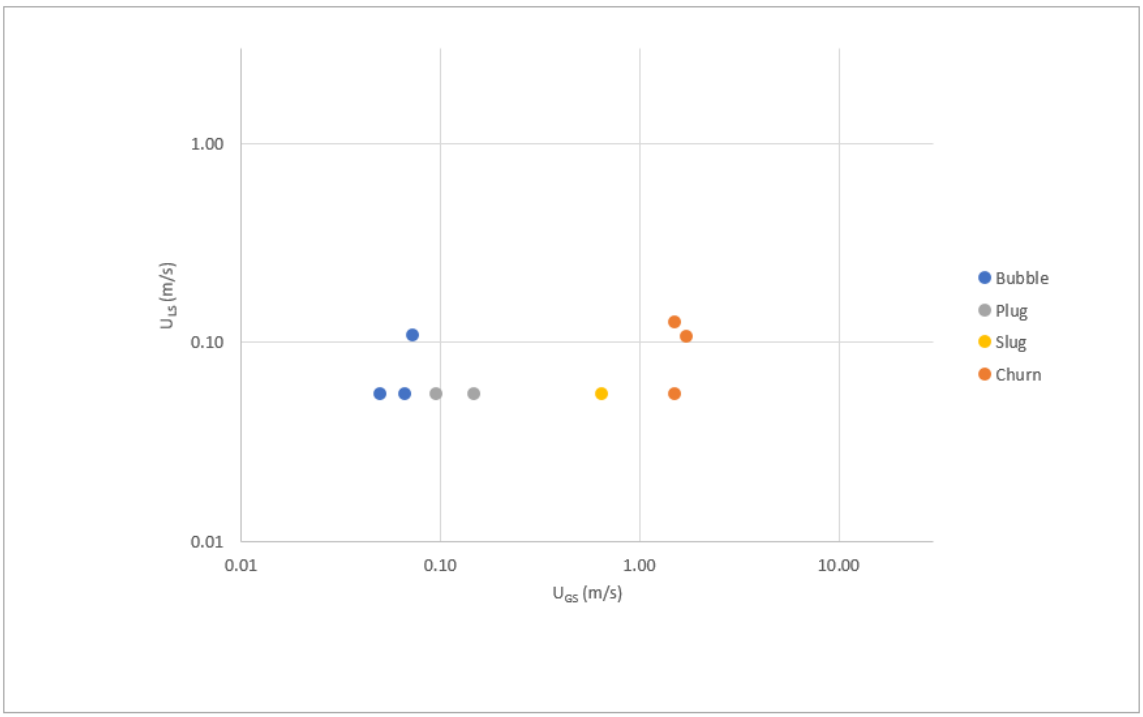

Figure 4.11: Flow Regime Map for Large Pump Connector (45°)

4.2.2: Flow Regime Characterization in Small Pump Connector

4.2.2.1: 0 Degrees (Vertical)

The same test was repeated for the small pump connector, but an unexpected disturbance occurred. During the down stroke, the fluid level in the outside tube-middle tube annulus rose significantly and eventually exited the device. This indicated a problem, because fluid level should remain constant or rise at a rate consistent with the injected fluids. This issue did not exist with the large pump connector.

Several attempts were made to troubleshoot this problem. The standing valve, traveling valve, stroke length and stroke rate were all adjusted. Finally, the water rate was reduced to try to prevent fluid from exiting the outside tube. This improved the issue, but diminished flow to rates not amenable to testing. As a result, the small pump connector did

not undergo further experimentation. This matter will continue to be investigated and hopefully resolved in Suresh's (2018) upcoming thesis.

4.3: DISCUSSION

Testing of the large pump connector revealed several important findings. As Figure 4.5 demonstrates, the flow regimes in the large pump connector at 0 degrees are consistent with those seen in literature. There was minor disparity between two of the classifications. Tests 4 and 5 were identified as bubble and churn flow in this research but as slug flow in Kelessidis and Dukler (1989). This discrepancy is most likely due to the ambiguity with the visual observation method and not actual differences between the flow regimes in this device and other vertical concentric annuli. This issue can be resolved by use of the conductivity probe method discussed prior.

There was also a difference between the flow regime at the bottom and top of this device, where turbidity appeared to increase with height. This is most likely an inlet effect and the result of the fluids mixing at the base of the outside tube. The fluid flow regime was characterized in the upper portion of this device, because it was felt that this region was more reflective of actual flow conditions. This prototype could be improved by mixing the fluids before they enter the device.

The air and water rates were kept as consistent as possible to permit comparison between the various inclinations. The tests at 10 and 20 degrees did not appear to have a remarkable effect on the fluid flow regime classification. The only noteworthy difference was the delayed onset of churn flow; churn flow was seen in Test 5 at 0 degrees, but Test 6 at 20 degrees. To the best of this author's knowledge, there are no published flow regime maps for concentric annular flow at 10, 20 and 45 degree inclinations. Original flow regime maps were generated for these cases.

A greater effect was seen when the device was positioned at 45 degrees. Plug flow, which is a horizontal flow regime, was identified in Tests 3 – 5. This regime presented with bullet-shaped bubbles at the top of the device. It was differentiated from slug flow, which had more round-shaped bubbles encompassing the entire annulus. In general, increased airflow was observed at the top of the device. This appeared to have a calming effect on the entire apparatus. Churn flow was delayed compared to the vertical orientation (Test 6 compared to Test 5) and was less severe. This agrees with the results at 20 degrees. This indicates that inclination delays the onset of churn flow up to 45 degrees. It also reduced the required stroke rate and appeared to improve the separating capacity of the device. These results are consistent with Bommer and Podio (2012), where the percentage of liquid entering the pump was greater than 95% at a 45 degree wellbore inclination. It should be noted that the placement of a beam pump in a 45 degree well is not recommended from a mechanical wear viewpoint.

Chapter 5: Conclusion

The flow regimes of a novel pump connector that doubles as a down-hole gas-liquid separator were discussed in this report. This is the first study of its kind. Two devices were built, a large and small pump connector, but only the large pump connecter was tested. The large pump connector exhibited flow regimes consistent with those seen in literature in its vertical orientation. Increasing the inclination up to 45 degrees delayed the onset of churn flow and appeared to improve the effectiveness of this device. Flow regime maps were generated at 10, 20 and 45 degree inclinations, but could not be compared to literature because no analogues were found. The small pump connector presented an issue, which was unable to be resolved before the completion of this report. Subsequent work can characterize its flow patterns when this issue is corrected. This research relied on visual observation to characterize the respective flow regimes. Future authors can refine these results by use of the conductivity probe technique. This work lays the foundation for Adi Suresh's Spring 2018 thesis that will discuss the separating capacity of this device. Classifying the fluid flow regimes was important because Suresh will investigate how flow regime can influence Bommer and Podio's (2012) guideline of keeping the liquid rate below 6 inches per second and whether this threshold is important at all. The down-hole separation of gas and creating enough discharge pressure to flow fluids to the surface are two widespread problems facing pump assisted wells. The pump connector is one possible solution to fill this void. A proper understanding of this device, especially the fluid flow within it, will aid in its improved application and design.

Nomenclature

$D_i = inner\ annulus\ diameter$

$D_{d,max} = maximum\ distorted\ bubble\ limit$

$D_o = outer\ annulus\ diameter$

$g = gravitational\ acceleration$

$ID_{ma} = internal\ diameter\ of\ mud\ anchor\ (in)$

$L = characteristic\ linear\ dimension$

$OD_{dt} = outer\ diameter\ of\ dip\ tube\ (in)$

$P_{ave} = average\ annulus\ perimeter$

$Re = Reynolds\ number$

$q_l = liquid\ capacity\ (bpd)$

$u = velocity\ of\ the\ fluid\ with\ respect\ to\ the\ object$

$U_G = gas\ bubble\ velocity$

$U_{GS} = superficial\ gas\ bubble\ velocity$

$U_L = average\ liquid\ velocity$

$U_{LS} = superficial\ average\ liquid\ velocity$

$v = kinematic\ viscosity\ of\ the\ fluid$

$V = measured\ voltage$

$V_{max} = maximux\ voltage\ for\ which\ a\ non-zero\ PDF\ value\ is\ estimated$

$\Delta\rho = density\ difference\ between\ two\ phases$

$\epsilon = void\ fraction$

$\mu = dynamic\ viscosity\ of\ the\ fluid$

$\rho = density\ of\ the\ fluid$

$\sigma = surface\ tension$

References

Bird, R. Byron, Stewart, Warren E., & Lightfoot, Edwin N. (2002). *Transport Phenomena* (2nd ed.). United States of America: John Wiley & Sons, Inc.

Bommer, Paul M. & Podio, A.L. (2012). *The Beam Lift Handbook* (1st ed.). United States of America: University of Texas at Austin.

Bommer, Paul M. & University of Texas at Austin (2014). A Novel Down-Hole Gas-Liquid Separator and Pump Connector. United States Patent and Trademark Office.

Cholet, Henri (2008). *Well Production Practical Handbook.* Paris, France: Éditions Technip.

Davies, R.M. & Taylor, G. (1950). The Mechanics of Large Bubbles Rising Through Extended Liquids and Through Liquids in Tubes. *Royal Society.*

Economides, Michael J., Hill, A. Daniel, Ehlig-Economides, Christine (1994). *Petroleum Production Systems.* Upper Saddle River, NJ: Prentice Hall PTR.

Hernández, Leonor, Julia, J. Enrique, Ozar, Basar, Hibiki, Takashi, & Ishii, Mamoru (2011). Flow Regime Identification in Boiling Two-Phase Flow in a Vertical Annulus. *Journal of Fluids Engineering*, *Vol. 133, 091304-1.*

Hewitt, G.F. & Hall-Taylor, N.S. (1970). *Annular Two-Phase Flow*. Oxford, England: Pergamon Press.

Kelessidis, V.C. & Dukler, A. E. (1989). Modeling Flow Pattern Transitions for Upward Gas-Liquid Flow in Vertical Concentric and Eccentric Annuli. *International Journal of Multiphase Flow, Vol 15, No. 2., pp. 173-191.*

Ishii, Mamoru & Hibiki, Takashi. (2011) *Thermo-Fluid Dynamics of Two-Phase Flow* (2nd ed.). New York: Springer.

Lea, James F. (2007). *Volume IV Production Operations Engineering.* Joe D. Clegg (ed.). *Petroleum Engineering Handbook.* Larry W. Lake (ed.-in-chief). United States of America: Society of Petroleum Engineers.

Matthews, Cam M., Zahacy, Todd A., Alhanati, Francisco J.S., Skoczylas, Paul, & Dunn, Lonnie J. (2007). *Volume IV Production Operations Engineering.* Joe D. Clegg (ed.). *Petroleum Engineering Handbook.* Larry W. Lake (ed.-in-chief). United States of America: Society of Petroleum Engineers.

Suresh, Adi. (2018). (Unpublished master's thesis). The University of Texas at Austin.

Winkler, Herald W. & Blann, Jack R. (2007). *Volume IV Production Operations Engineering.* Joe D. Clegg (ed.). *Petroleum Engineering Handbook.* Larry W. Lake (ed.-in-chief). United States of America: Society of Petroleum Engineers.